FEATURE EXTRACTION OF OCEANIC INTERNAL WAVES BASED ON REMOTE SENSING IMAGERY

Chih-Chung Kao, Assistant Prof.
Department of Information Management
Fortune Institute of Technology
14FL, 62 Chien-An St., San-Min Dist.,
Kaohsiung, Taiwan, R.O.C.
kcc7879@cneter.fotech.edu.tw

Ming-Jer Huang, PhD Candidate
Department of Marine-Engineering
National Sun Yet-San University
70 Lien-hai Rd. Kaohsiung, Taiwan R.O.C.
d9054807@student.nsysu.edu.tw

Ying-Jang Yang, Associate Prof.
Department of Marine Science
Chinese Naval Academy
P.O.BOX 90175 Tsoying, Taiwan R.O.C.
yjyang@can.edu.tw

ABSTRACT

Oceanic internal waves play an important role in fishing activities and the safety of oil drilling platforms, as well as the navy's antisubmarine warfare (ASW) and the safety of submarines. Due to its characteristics of relatively all weather capability, Synthetic Aperture Radar (SAR) images became popular in observing the appearance of oceanic internal waves recently. The purpose of this study is to develop a methodology and a computer assisted tool to extract features of internal waves based on SAR imagery using spatial information techniques including digital image processing, wavelet transform, and geographic information analysis. Among the methods of feature extraction, edge detection will be the primary method for extracting features of oceanic internal waves. Thus, methods of Canny, WTMM (Wavelet Transform Modulus Maxima), and Wavelet Correlator will be implemented and investigated for selecting a proper edge detector. The developed tool will then be applied to extract features of the internal waves in the northern South China Sea. Integrating the extracted features and the in-situ observations in a geographic information system (GIS), the dynamics of the internal waves can be better understood. The automated process of extracting features of oceanic internal waves show significant time saving compared to the traditional manual operation.

INTRODUCTION

Remote sensing techniques are capable of detecting the sea surface roughness caused by oceanic internal waves, which can then be applied to analyze the dynamics of internal waves in a wide range of ocean area. Due to its characteristics of relatively all weather capability, we are able to observe the appearance of oceanic internal waves based on Synthetic Aperture Radar (SAR) images. Our specific research interest is focused on the internal waves in the northern South China Sea due to its rich activities (Yang *et al.*, 2004). The long-term research objective is to study the temporal and spatial dynamics of internal waves in the study area based on the extracted features of internal waves and in-situ measurements, in order to derive for the dynamic behaviors of the internal waves. To study the dynamics of the internal waves from a generation phase to a propagation phase and then to a dissipation phase, the feature database and the in-situ data need to be integrated in support of finding the evolving behavior of the internal waves.

Oceanic internal waves play an important role in fishing activities and the safety of oil drilling platforms, as well as the navy's antisubmarine warfare (ASW) and the safety of submarines. Integrating the extracted features and the in-situ observations in a geographic information system (GIS), the dynamics of the internal waves can be better understood. The purpose of this study is to develop a proper methodology and a computer assistant tool to extract features of internal waves from satellite imagery using spatial information analysis techniques including digital image processing, wavelet signal processing, and geographic information analysis. The system is developed in an object-oriented approach for image processing based on the C# language in Microsoft .NET Framework. We decided to apply the C# language of Microsoft .NET Framework for the system because of its compatibility to the C++ language of most image processing codes and its powerful GUI design environment. In this manner, our previous work in image processing can easily be adapted and integrated into an efficient C# GUI environment.

Edge detection plays an important role in pattern recognition fields, because edge is an important feature for identifying objects in images (Gonzalez and Woods 1992). Edge points are usually localized in the sharp change area of image intensity, which usually provide the information of object boundary. Many approaches have been developed to identify edge including first derivative filter, such as Sobel and Prewitt methods. Canny (1986) derived an optimal edge detector in a computational approach that aimed to minimizing edge detection error rate and location error. The singularity detection approach based on wavelet transform is inspired from Canny's edge detector (Mallat and Hwang, 1992). The other wavelet-based method, Wavelet Correlator (Kuo and Chen, 2003), will also be investigated.

In this paper, we will provide some background of internal waves. Then, we discuss the methods of edge detection in the following sections, and compare their effectiveness in edge detection, based on a case study of extracting features of internal waves, for better selecting the feature extractor for our system.

BACKGROUND AND METHOD

Internal Wave

Oceanic internal waves are waves that travel within the interior of the ocean. The internal waves may be generated by several sources including tidal flow, frontal boundaries, and special atmospheric conditions (Apel, 1987). When the internal waves flow over underwater obstacles, such as seamounts, shelf breaks, and troughs, they tend to become particle-like with large amplitudes within several kilometers, which is called solitary waves (Zabusky and Kruskal, 1965). One of the very early interests in studying these waves was the unexpectedly large shear stress when they impacted on offshore oil-drilling facilities (Bole *et el.*, 1994).

The Synthetic Aperture Radars (SARs) on ERS and Radarsat are sensitive to the sea surface roughness in a small scale, which is modulated by the velocity field of internal solitary waves (Figure 1). In the literature, most studies of solitary waves applying satellite imagery are focused on Synthetic Aperture Radar (SAR) (Apel, 1987; Liu *et al.*, 1998; Hsu *et al.*, 2000). Compared to the visible satellite imagery, SAR imagery is relatively unaffected by clouds and weather, and it is also of day/night operation, which makes it an effective vehicle for studying internal solitary waves.

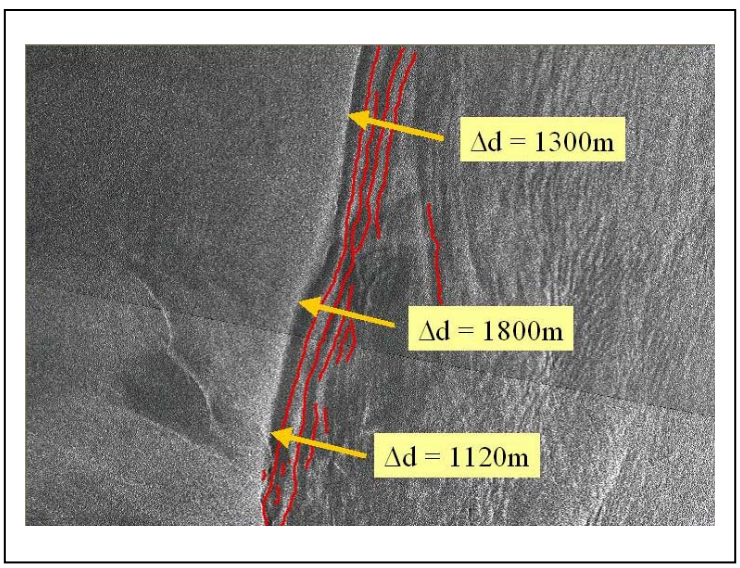

Figure 1. Comparison of two SAR images with a time interval of 28 minutes. The internal wave features extracted from the earlier image, shown with the red lines, are overlapped with the second image in the ESRI/ArcView 9.1 GIS software, for studying their motion dynamics.

Feature extraction of internal solitary waves based on SAR images can be effective due to its nearly all-weather capability. Figure 1 shows the comparison of two SAR images with a 28 minute time interval. The internal wave features extracted in the earlier image, shown with the red lines, can be overlapped with the second image for studying their motion dynamics. In the following sections we will discuss the methods of feature extraction in SAR imagery.

Wavelet Based De-speckle

The major concern of image processing using SAR imagery is the presence of speckle noise, which is usually scattered with bright and dark spots. These speckle noises occur with such radiation due to destructive superposition of reflected components with differing phase delays such as ultrasound, laser, and SAR images. Traditional Statistic filters, such as, Lee, Kuan, and Frost Filters tend to smooth noise while blurring important features and textures in the image. Donoho (1995) showed how wavelet transforms may be used to optimally de-noise. The merit of the wavelet based de-noise method is the edge preservation capability that comes from the localizability of the wavelet function. However, classical Discrete Wavelet Transform (DWT) suffers a drawback of shift variance results from the use of down-sampling in the DWT, which can lead to artifacts in wavelet de-noising results. Coifman and Donoho (1995) suggested that combing Hard Thresholding and Translation Invariance wavelet transform might provide better visual quality of de-noised images.

Multiscale Retinex (MSR) Method for Image Enhancement on High Dynamic Range Image

Modern satellite images posses a high dynamic intensity range with a 16-bit pixel level, such as ERS2/SAR, ASAR, and MODIS images. This dynamic range in pixel value is inconsistent with most computer visual output equipments with only an 8-bit pixel level display capability. The Multiscale Retinex (MSR) method provides a plausible approach to compress the dynamic range. Retinex is a human based image-processing algorithm, which provides color consistency and dynamic range compression (Daniel and Rahman, 1997a; 1997b). The single-scale retinex is given as:

$$R_i(x,y) = \log I_i(x,y) - \log\left[F(x,y) * I_i(x,y)\right], \qquad \text{(Eq1)}$$

where $R_i(x, y)$ is the retinex value, $I_i(x, y)$ is the image pixel intensity in the ith spectral channel, * denotes the spatial convolution operation, $F(x, y)$ is the Gaussian surround function

$$F(x,y) = Ke^{\frac{-r^2}{c^2}}, \qquad \text{(Eq2)}$$

where c is the scale factor, and factor K such that

$$\iint F(x,y)\,dxdy = 1. \qquad \text{(Eq3)}$$

The MSR is the weighted sum of each single-scale retinex

$$R_{MSR_i} = \sum w_n R_{n_i}, \qquad \text{(Eq4)}$$

where N is the number of scales, R_{ni} is the ith component of the nth scale, and w_n is the weight associate with the nth scale. The choice of scale c is based on the experimentation, where the small values of c provide good dynamic range compression and high details, but weak tonal and color rendition. The Multiscale retinex integrates the strength of each scale and prevents the weakness of each scale. The final MSR output can be calculated by using a "canonical" gain/offset to map between the retinex and the display range of output equipment (Daniel and Rahman, 1997b).

Canny Optimal Edge Detector

The most common method for edge detection is the magnitude of the first derivative of local gray-level $f(x,y)$ in an image. The magnitude $Mf(x,y)$ of edge signal can be derived as:

$$Mf\,(x,y)=\sqrt{\left(\frac{\partial f}{\partial x}\right)^2+\left(\frac{\partial f}{\partial y}\right)^2}\ , \qquad \text{(Eq5)}$$

where f/ x and f/ y is the first derivative of *f(x,y)* in the *x* and *y* directions.

In practice, the first derivative f/ x and f/ y in the *x* and *y* directions can be approximated using a spatial mask, such as Sobel, Prewitt, and Kirsch Filters for convenience. The drawback of these operators is that they are sensitive to noise, especially that in satellite images, resulting from image acquisition systems and the radiation environment in nature. Edge pixels in an image can be identified by setting a threshold to filter out the non-edge points.

Canny (1986) derived an optimal operator for edge detection based on three criteria. The first criterion is low error rate, where image edges should not be missed by the operator. The second criterion is that the edge points should be well localized with minimized offset from the true edge. The third criterion is that the operator should have only one response to a single edge. Based on these criteria, his approach defines edge points as a local maximum of the first derivative of a Gaussian smooth filter G_n applied to the image *f(x,y)*. At the local maximum, the derivative

$$\frac{\partial}{\partial n}G_n * f\,(x,y)=0\ , \qquad \text{(Eq6)},$$

where *n* is the directional vector, and * is an operator of spatial convolution. In practice, the edge strength can be calculated as the magnitude of the convolution between the first derivative of a Gaussian smooth filter and the image *f(x,y)* for convenience. The method then suppresses any pixel that is not an edge point. Finally, the Hysteresis process is used to filter the remaining points with two thresholds, such that the higher threshold identifies strong edge pixels and the lower threshold preserves weak edge pixels connecting to the strong edge pixels.

Wavelet Transform Modulus Maxima (WTMM)

Mallat and Hwang (1992.a, .b) proved that the local maxima of the dyadic wavelet transform modulus can characterize the local structure of signals, which then indicates the location of edges in an image. The wavelet transform modulus *Mf(x,y)* can be expressed as:

$$M_j\, f\,(x,y)=\sqrt{\left|W_j^{\,1} f\,(x,y)\right|^2+\left|W_j^{\,2} f\,(x,y)\right|^2}\ , \qquad \text{(Eq7)}$$

where $W_1 f(x,y)$ is the dyadic wavelet transform of image pixel intensity in the *x* direction, and $W_2 f(x,y)$ is the dyadic wavelet transform of image pixel intensity in the *y* direction. The direction of the modulus is given as:

$$A_j\, f\,(x,y)=\arctan\left[\frac{W_j^1 f\,(x,y)}{W_j^2 f\,(x,y)}\right]\ . \qquad \text{(Eq8)}$$

Edge pixels in an image can be identified by chaining the modulus maxima along the modulus direction of pixel intensity. We named this method WTMM in this paper.

Wavelet Correlator (WTC)

Kuo and Chen (2003) proposed another edge detection method in the wavelet transform domain. They defined the wavelet correlator as *R(l, x, y)* to incorporate the wavelet coefficient in each decomposed level *j*

$$R(l,x,y)=\prod_{j=0}^{l-1} M_j\, f\,(x,y)\ , \qquad \text{(Eq9)}$$

where the wavelet modulus is defined as

$$M_j f(x,y) = \sqrt{\left|W_j^{\,1} f(x,y)\right|^2 + \left|W_j^{\,2} f(x,y)\right|^2 + \left|W_j^{\,3} f(x,y)\right|^2}\ , \quad \text{(Eq10)}$$

where, $W_j^1 f(x,y)$ is the wavelet transform of image pixel intensity in the *x* direction, $W_j^2 f(x,y)$ is the wavelet transform of image pixel intensity in the *y* direction, and $W_j^3 f(x,y)$ is the wavelet transform of pixel intensity in the diagonal direction. The edge points can be determined by thresholding the correlator.

Feature Extraction Tool Development

Our feature extraction system for internal waves is developed in an object-oriented approach for image processing based on the C# language in Microsoft .NET Framework. Figure 1 shows the workflow of the system functionality. Beside the basic image operation functions, the system currently has three major modules. The first module includes image de-noise and MSR image dynamic range compression, followed by edge detection, then feature vectorization. Finally, the extracted features of internal waves can be displayed and overlapped with other spatial information in GIS software.

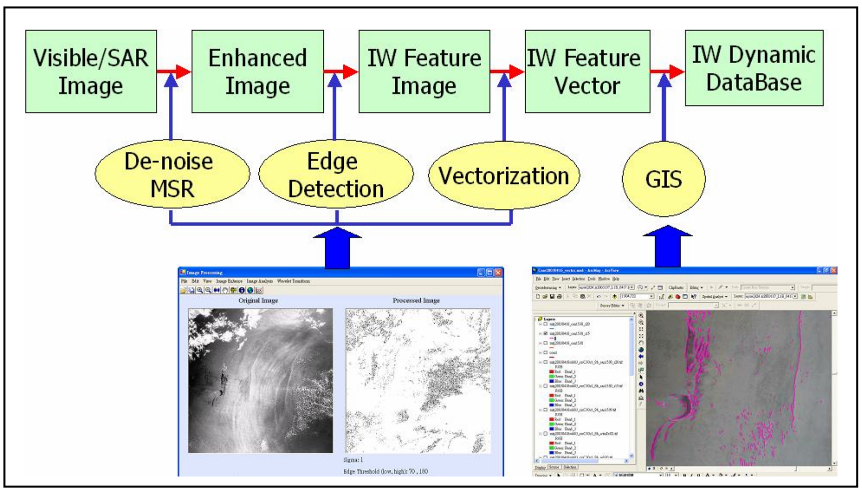

Figure 2. The workflow of the feature extraction tool.

EXPERIMENTS

Study area: Luzon Strait to Hainan Island

The research activities in this area have been active in recent years. Internal solitary wave are observed most frequently in the months between April and September (Apel, 1987; Liu *et al*., 1998; Hsu *et al*., 2000). The ASAR image used in this experiment was taken on 16-APR-2003, 02:14. The image is centered at 117-20E and 20-50N where the lagoon around Tung-Sha Island is located on the lower left corner. Figure 3(a) shows the original SAR image with a 16-bit intensity level. Our primary research interest is focused on the internal waves in the northern South China Sea due to its rich activities (Yang *et al*., 2004). The long-term research objective is to study the temporal and spatial dynamic of internal waves in the study area based on the extracted features of internal waves and in-situ measurements, in order to derive for the dynamic behaviors of the internal waves.

SAR Image De-speckle and Enhancement

In this experiment, we studied the effectiveness of the MSR method to enhance an ASAR image. Image 3(a) shows the original ASAR image with a 16-bit intensity level. The side-looking natural of SAR imagery normally displays a dark tonal change gradually from the near-side to the far-side, which results in a lower visibility in the image on the far-side. Therefore, the quality of feature extraction in this area is degraded. Image 3(b) is the detected edge image based on the Canny method, and Image 3(c) is the result of length thresholding of 25 pixels on Image 3(b). Due to the lower visibility on the far-side (left side) of the original image, features extracted in this area are sparse. We applied the MSR method on image 3(a), and image 3(d) is the enhanced image where sea surface features are clear. Images 3(e) and 3(f) are the detected edge images in the scene based on the Canny method, and then edge length thresholding of 25 pixels, respectively, where spatial features of internal waves and surface waves are clearly identified. Comparing images 3(c) and 3(f), the feature extraction based on the MSR enhanced image shows better results than that of the original image.

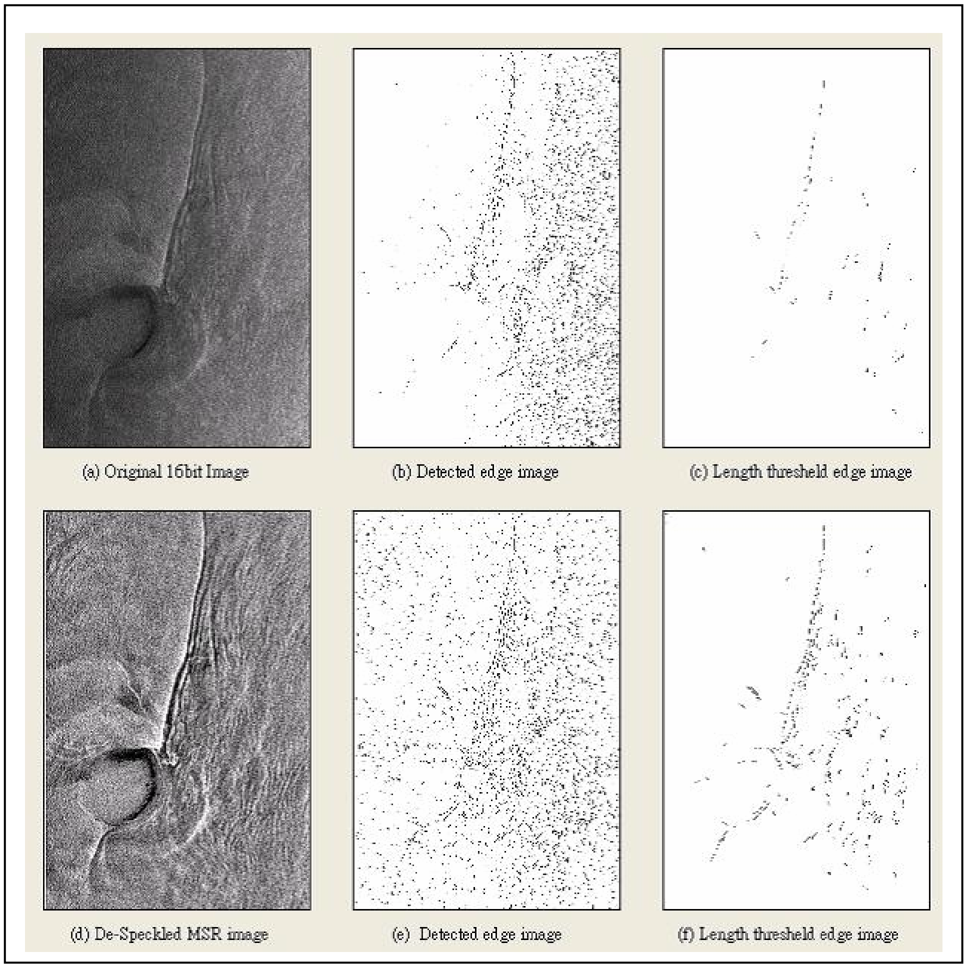

Figure 3. ASAR Image De-speckle and Enhancement. Image (a) is the original ASAR image with a 16-bit intensity level. Images (b) and (c) are the detected edge images in the scene based on the original image using the Canny method, and then edge length thresholding, respectively. Image (d) is the dynamic range compressed image based on MSR method. Images (e) and (f) are the detected edge images in the scene based on the dynamic range compressed image using the Canny method, and then edge length thresholding, respectively.

Edge Detection

In this experiment, we compared the effects of feature extraction based on different methods. We applied the Quadratic Spline wavelet function suggested by Mallat (1998) on both WTMM and WTC methods. On the other hand, we also applied the bi-orthonormal Daubechies 97 (D97) wavelet function on both WTMM and WTC methods. Daubechies 97 (D97) wavelet function is the standard wavelet function used in the format of JPEG200. In the experiment, we conducted Canny, D97WTMM, D97WTMM, D97WTC, and D97WTC edge detection cases on the MSR enhanced image. Image 4 shows the results of each edge detection method. Among them, the classical Canny method outperforms other methods in terms of the detected quantity of features. We will discuss the quality of feature extraction in the next section. The WTMM method using Quadratic Spline wavelet function seems to be better than those using Daubechies 97 wavelet function. The methods of Canny and WTMM, searching the edge points along the local maximum of the intensity slope, detect edges with the width of a single pixel, which is better than the intensity thresholding method of WTC which normally produces thick edges.

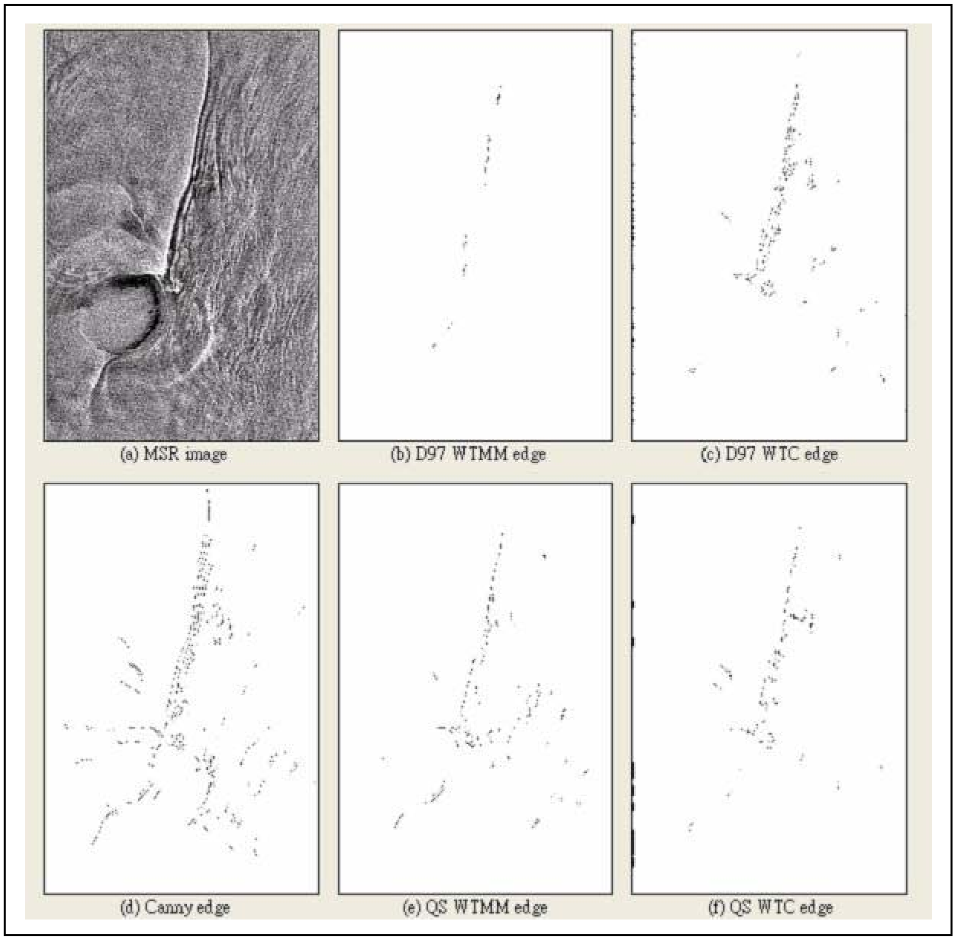

Figure 4. Comparison of Edge Detection. The effects of feature extraction based on different methods are compared. The classical Canny method shows better result against other methods.

DISCUSSION

Edge detection plays an important role in feature extraction, because edge is an important feature for identifying objects in images. Edge points are usually localized in the sharp change area of image intensity, which usually provides the information of object boundary. Furthermore, the localization quality of edge detectors is important especially for the spatial information related research when the position is demanded.

In Figure 5, the detected features of internal waves were converted in a vector form; therefore, it can be overlapped with the original image in the ERSI/ArcView 9.1 software base on the same geographic coordinates reference. Figure 5 shows the vectorized feature of the internal waves extracted using the Canny method with the Gaussian factors of sigma = 1, 2, 3, and 4 in purple, yellow, red, and green colors, respectively. The quality of the localization of feature extraction can be measured in the GIS software, which is within one pixel variation. Figure 6 shows the quality of localization of WTMM method using Quadratic Spline wavelet function. The red line is the feature extracted by the Canny method, while the yellow, blue, and green lines are the features extracted by the WTMM method in the wavelet decomposition level of j = 2, 3, and 4, respectively. The deviations between the locations of the extracted features from the true feature boundary are 2, 4, and 8 pixels, which is surprisingly unexpected. We also compared the localization error of the other methods in Table 1, which also shows that the classical Canny method outperforms other methods in terms of the quality of localization.

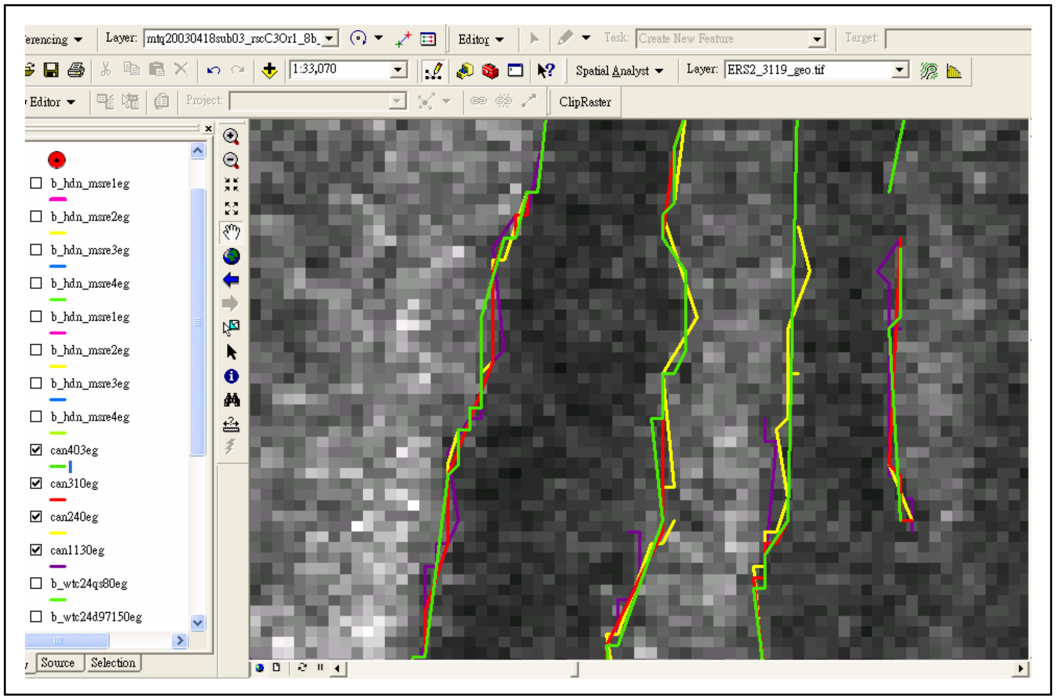

Figure 5. Vectorized features of the internal waves extracted using the Canny method with sigma = 1, 2, 3, and 4 in purple, yellow, red, and green colors, respectively. The quality of its localization is within one pixel variation.

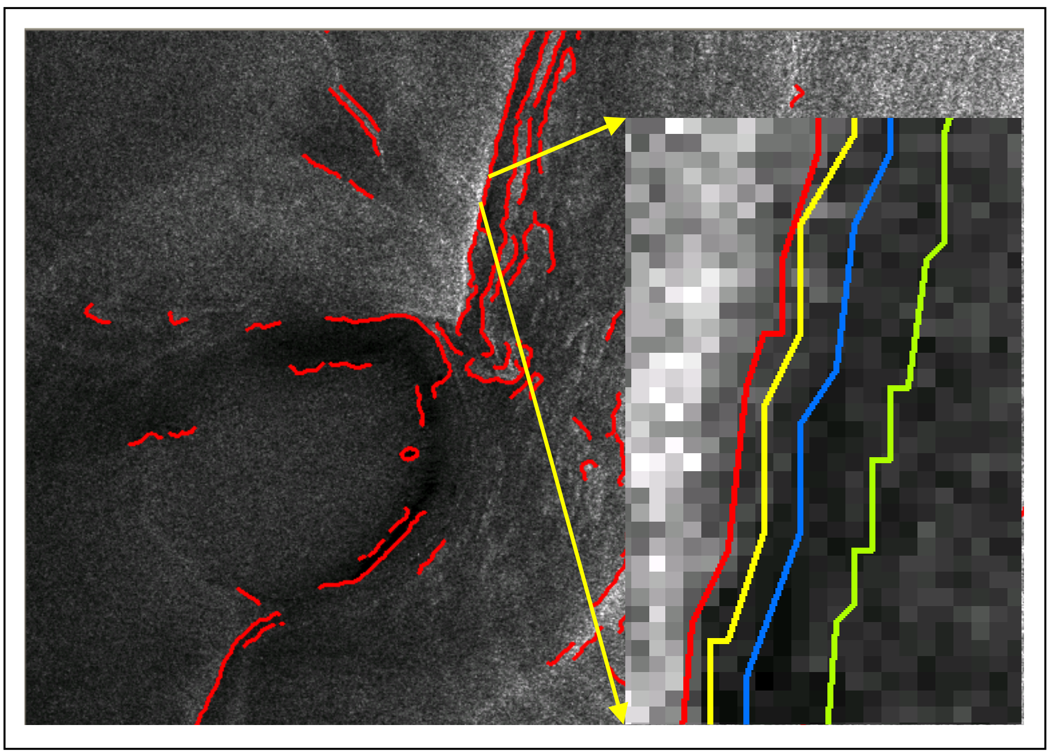

Figure 6. The quality of localization with the WTMM method using Quadratic Spline wavelet function. The red line is the feature extracted by the Canny method, the yellow, blue, and green lines are the features extracted by the WTMM method in the decomposition level of j = 2, 3, 4, respectively.

Table 1. The localization error of each feature extraction method in pixels.

Feature Extraction Method	Canny	Q-Spline WTMM	D97 WTMM	Q-Spline WTC	D97 WTC
1 (sigma/level)	< 1	< 1	-2	2	1
2 (sigma/level)	< 1	2	-1	N/A	N/A
3 (sigma/level)	< 1	4	1	N/A	N/A
4 (sigma/level)	< 1	8	2	N/A	N/A

CONCLUSION

In this study, we implemented different methods for the feature extraction of internal waves using SAR imagery, which is complicated due to its nature of side-looking and destructive superposition of reflection. Therefore, we applied methods of Translation Invariance wavelet transform and Hard Thresholding to avoid the de-speckle artifacts and preserve the signal of edges and texture in the SAR image. Comparing the result of feature extraction using different methods, the classical Canny method outperforms the other methods both in quality and quantity. The method of wavelet based methods show poor localizability in detecting the true boundary of internal waves, which shows a need of further studies to investigate the localizability issues of wavelet methods in pattern recognition.

.

ACKNOWLEDGEMENT

This study was mainly supported by the National Science Council of R.O.C. (NSC 94-2611-M-268-001: Extracting Features of Internal Waves Using Satellite Imagery and Spatial Information Techniques).

REFERENCE

Apel, John R. (2002). Oceanic Internal Waves and Solitons, *An Atlas of Oceanic Internal Solitary Waves* (May 2002) , Prepared for Office of Naval Research.

Bole, J.B., C. C. Ebbesmeyer, and R.D Romea (1994). Soliton currents in the South China Sea: Measurements and Theoretical Modeling, *Proc. 26th Annual Offshore Technology Conf.*, Houston, TX, 367-376.

Canny, John (1986). A Computational Approach to Edge Detection, *IEEE Transactions on Pattern Analysis and Machine Intelligence*, PAMI-8(6):679-698.

Coifman, R.R. and D.L. Donoho (1995), Translation Invariant De-noising, *Lecture Notes in Statistics*, 103:125-150.

Daniel J. J. and Z. Rahman (1997a). Properties and Performance of a Center/Surround Retinex, *IEEE Transactions On Image Processing*, 6(3): 451-462.

Daniel J. J. and Z. Rahman (1997b). A Multiscale Retinex for Bridging the Gap Between Color Images and the Human Observation of Scenes, *IEEE Transactions On Image Processing*, 6(7):965-976.

Daubechies I. (1992). *Ten Lectures on Wavelets*. CBMS series. Philadelphia: SIAM.

Donoho, D. L. (1995). De-noising by Soft Thresholding. *IEEE Transaction on Information Theory*, 41(3): 613-627.

Ebbesmeyer, C. C., C. A. Coomes, R. C. Hamilton, K. A. Kurrus, T. C. Sullivan, B. L. Salem, R. D. Romea, and R. J. Bauer (1991). New Observations on Internal Waves (Solitons) in the South China Sea using an Acoustic Doppler Current Profiler, *Marine Technology Society 91 Proceedings*, New Orleans, 165-175.

Gonzale, R. C. and Woods, R. E. (1992). *Digital Image Processing*, Addition-Wesley Publishing Company, Inc. Reading, Massachusetts.

Goswami, J.C. and A.K. Chan (1999). *Fundamentals of Wavelets: Theory, Algorithms, and Applications*. Wiley-Interscience, New York.

Hsu, M.K., A. K. Liu, and C. Liu (2000): A study of Internal Waves in the South China Seas and Yellow Sea using SAR. *Cont. Shelf Res*., 29: 389-410.

Kuo, J. M. and K. S. Chen (2003). The Application of Wavelets Correlator for Ship Wake Detection in SAR Images, IEEE Trans. *Geoscience and Remote Sensing*, 41(6): 1506-1511.

Liu, A. K. Y. S. Chang, M.K. Hsu, and N. K. Liang (1998). Evolution of Nonlinear Internal Waves in the China Seas, *J. Geophys. Res*., 103: 7995-8008.

Mallat, S.G. (1989). “A Theory for Multiresolution Signal Decomposition: The Wavelet Representation,” *IEEE Transactions on Pattern Analysis and Machine Intelligence*, 11(7): 674-693.

Mallat, S.G. and Zhong, S. (1992.a). Characterization of Signals from Multiscale Edges, *IEEE Transactions on Pattern Analysis and Machine Intelligence*, 14(7): 710-732.

Mallat, S.G and Hwang, W.L. (1992.b). Singularity Detection and Processing with Wavelets, *IEEE Transactions on Information Theory*, 38(2): 617-643.

Mallat, S.G. (1998). *A Wavelet Tour of Signal Processing*, San Diego: Academic Press.

Yang, Y. Y., T. W. Tang, M. H. Chang, A. K. Liu, M.K. Hsu, and S. R. Ramp (2004). Solitons Northeast of Tung-Sha Island during the ASIEX Pilot Studies, *IEEE Journal of Oceanic Engineering*, 29(4):1182-1199.

Zabusky, N.J. and M. D. Kruskal. (1965) Inteaction of "Solitions" in a Collisionless Plasma and the Recurrence of Initial State, *Phys. Rev. Lett.*, 15(6): 240-243.